Spin-resolved photoemission study of epitaxially grown $MoSe_2$ and WSe_2 thin films

2016 J. Phys.: Condens. Matter 28 454001

(http://iopscience.iop.org/0953-8984/28/45/454001)

IOP Publishing Journal of Physics: Condensed Matter
J. Phys.: Condens. Matter **28** (2016) 454001 (7pp) doi:10.1088/0953-8984/28/45/454001

Spin-resolved photoemission study of epitaxially grown $MoSe_2$ and WSe_2 thin films

Sung-Kwan Mo[1], Choongyu Hwang[2], Yi Zhang[1,3,4], Mauro Fanciulli[5,6], Stefan Muff[5,6], J Hugo Dil[5,6], Zhi-Xun Shen[4,7] and Zahid Hussain[1]

[1] Advanced Light Source, Lawrence Berkeley National Laboratory, Berkeley, CA 94720, USA
[2] Department of Physics, Pusan National University, Busan 609-735, Korea
[3] National Laboratory of Solid State Microstructures, School of Physics, Collaborative Innovation Center of Advanced Microstructures, Nanjing University, Nanjing 210093, People's Republic of China
[4] Stanford Institute of Materials and Energy Sciences, SLAC National Accelerator Laboratory, Menlo Park, CA 94025, USA
[5] Institut de Physique, Ecole Polytechnique Fédérale de Lausanne, CH-1015 Lausanne, Switzerland
[6] Swiss Light Source, Paul Scherrer Institut, CH-5232 Villigen, Switzerland
[7] Geballe Laboratory for Advanced Materials, Departments of Physics and Applied Physics, Stanford University, Stanford, CA 94305, USA

E-mail: SKMo@lbl.gov

Received 14 April 2016, revised 26 July 2016
Accepted for publication 15 August 2016
Published 12 September 2016

Abstract

Few-layer thick $MoSe_2$ and WSe_2 possess non-trivial spin textures with sizable spin splitting due to the inversion symmetry breaking embedded in the crystal structure and strong spin–orbit coupling. We report a spin-resolved photoemission study of $MoSe_2$ and WSe_2 thin film samples epitaxially grown on a bilayer graphene substrate. We only found spin polarization in the single- and trilayer samples—not in the bilayer sample—mostly along the out-of-plane direction of the sample surface. The measured spin polarization is found to be strongly dependent on the light polarization as well as the measurement geometry, which reveals intricate coupling between the spin and orbital degrees of freedom in this class of material.

Keywords: transition metal dichalcogenides, $MoSe_2$, WSe_2, spin-resolved photoemission, ARPES, photoemission

(Some figures may appear in colour only in the online journal)

1. Introduction

Two-dimensional (2D) materials, such as graphene, hBN, phosphorene, and transition metal dichalcogenides (TMDCs), are the platform for new physical properties that are not attainable in their bulk counterparts [1–4]. They often exhibit a versatile electronic structure controllable by thickness, surface chemical adsorption, and strain [5–7]. They can also be stacked into heterostructures to develop a new state in the interfaces [8] as well as through the proximity effect [9]. Of particular interest is the TMDC, MX_2 (M = Mo, W; X = S, Se) semiconductor with unique properties in the few-layer limit, such as indirect to direct band gap transition [10, 11], large exciton binding energy [12–14], well-defined valley degrees of freedom [15–18], and spin-splitting of the valence band (VB) [19–21]. Many efforts have been made to harvest these properties into practical optoelectric, spintronic, and valleytronic devices [22–24].

The hallmark of the electronic structure of MX_2 is the spin-splitting of the VB at the K/K′-point of the hexagonal Brillouin zone and concomitant spin-valley locking [14–16, 20]. A single layer of MX_2 is made of a layer of M atoms in a trigonal prismatic coordination sandwiched by two layers of X atoms. When the thickness is reduced to a single layer (1 ML), the inversion symmetry is naturally broken. Combined with strong spin–orbit coupling (SOC), this leads to sizable Rashba-type spin-splitting as well as strong spin-valley coupling with distinct real spin indices at the K/K′-point [17].

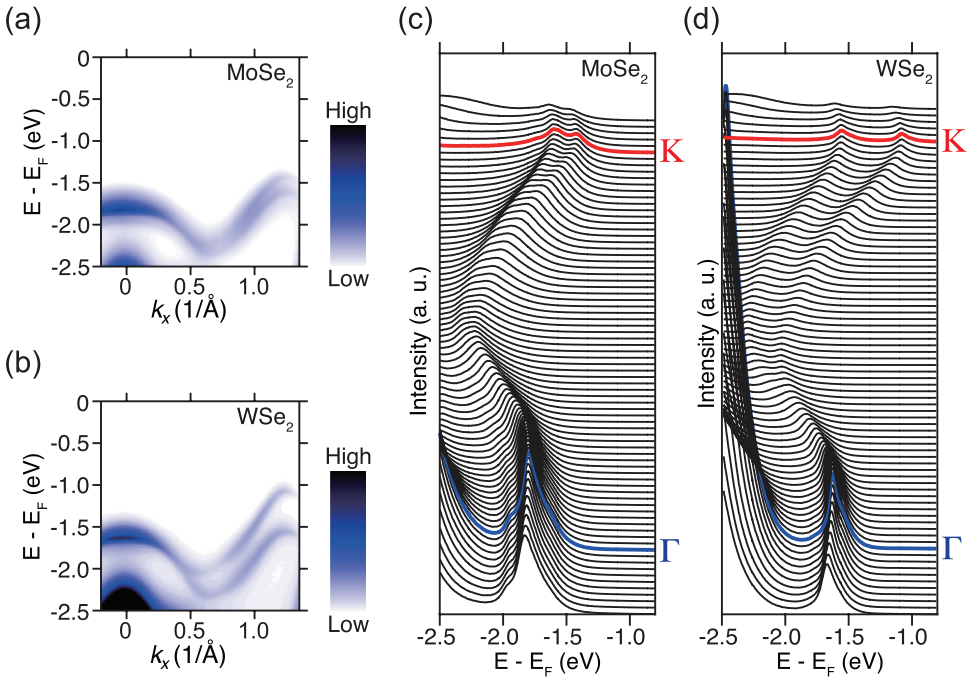

Figure 1. The spin-integrated ARPES spectra of 1 ML $MoSe_2$ and WSe_2 measured with 70 eV photons at 60 K. (a), (b) The intensity map along the Γ-K direction of the hexagonal Brillouin zone. (c), (d) EDC stacks along the same direction. Both show the monolayer features at the Γ-point and clear splitting at the K-point.

Inversion symmetry is recovered in bilayer (2 ML) making the VB spin-degenerate. With trilayer (3 ML) thickness, the inversion symmetry is broken again, but with less pronounced spin polarization compared to that in 1 ML [20].

Angle-resolved photoemission spectroscopy (ARPES) is one of the most suitable tools for investigating the electronic structure of 2D materials with energy and momentum resolution as well as surface sensitivity [25]. There have been a number of ARPES studies either on bulk MX_2 samples [26–28] or few-layer samples [20, 21, 29, 30] prepared by various methods such as exfoliation, chemical vapor deposition (CVD), and epitaxial growth. They all observe sizable splitting in the VB at the K-point, with a size of ∼170 meV for MoS_2 and $MoSe_2$ and ∼450 meV for WS_2 and WSe_2 as W induces larger SOC. However, due to the spin-integrated nature of their spectra, one cannot really conclude that these are spin-split bands purely from the experimental data unless supported by theoretical calculations. In addition, the nature of the spin texture of each band cannot be deduced.

The additional information on spin polarization can be obtained through spin-resolved ARPES (SARPES) [31–33], as has been shown for topological surface states in topological insulators [34–36]. There have only been a few SARPES studies on MX_2 [37–39], despite the large interest in this material class, mainly due to the difficulty in preparing the large-area samples suitable for measurements in ultra-high vacuum environments. This is because current SARPES setups at the synchrotron sources must have a large beam spot size to allow maximum photon flux. Moreover, previous SARPES works have all still essentially been on bulk samples of MX_2, such as the bulk inversion symmetry broken 3R phase of MoS_2 [37] or spin polarization induced by the space charge residing in the overlayer [38]. Of particular interest, Riley *et al* [39] report on the spin-polarized signal from a regular bulk WSe_2, and interprets the results in terms of strong electron localization at the K/K′-point of WSe_2.

In this paper, we present the SARPES data measured on few-layer $MoSe_2$ and WSe_2 samples, grown by molecular beam epitaxy (MBE) on a bilayer graphene (BLG) substrate with exact layer-by-layer thickness control. We found that the spin polarization lies mostly in the out-of-plane direction of the sample surface in the 1 ML samples of both $MoSe_2$ and WSe_2, albeit the degree of polarization is not as much as proposed by the theory. The spin polarization disappears and reappears as the thickness increases to 2 MLs and 3 MLs following the recovery and breaking of the inversion symmetry. We only found the valley-dependent spin flip between the K and K′ points in a particular geometry, which indicates the existence of non-trivial geometric effects in our SARPES signal. We also found a light polarization-dependent flip of spin polarization due to the intricate coupling between the spin and orbital degrees of freedom.

2. Experimental

Thin film samples of $MoSe_2$ with 1 ML, 2 ML and 3 ML thicknesses and WSe_2 with 1 ML thickness were grown using MBE on a bilayer graphene substrate at the Beamline 10.0.1, Advanced Light Source, Lawrence Berkeley National Laboratory. The number of layers, the crystallographic phase, and the surface quality were monitored using reflection high-energy electron diffraction (RHEED), low-energy electron diffraction (LEED), and *in situ* spin-integrated ARPES. The details of the growth condition and the sample characterization were the same as described in [20] and [21]. The samples were

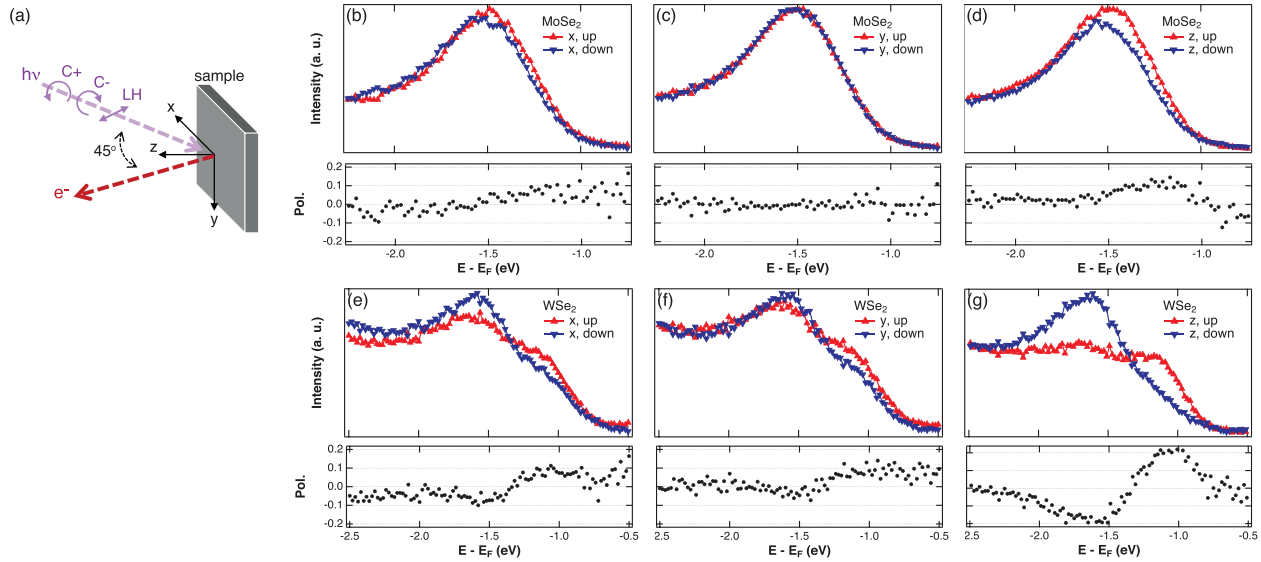

Figure 2. (a) A schematic diagram to show the measurement geometry. (b)–(d) The SARPES EDC intensity and polarization of 1 ML $MoSe_2$ along the x, y, and z directions at the K-point. (e)–(g) SARPES EDC intensity and polarization of 1 ML WSe_2 along the x, y, and z directions at the K-point.

then capped with amorphous Se with a thickness of ∼100 Å for the transfer to the SARPES system.

The SARPES measurements were performed at the COPHEE endstation of the SIS beamline at the Swiss Light Source, equipped with an Omicron EA125 analyzer and a pair of orthogonally mounted 40 kV Mott detectors [40]. The sample temperature and the base pressure were 20 K and 3×10^{-10} mbar, respectively. The Se capping layer was removed by heating the sample to 300 °C for 30 min right before the measurement. The absence of residual Se was confirmed by measuring the ARPES intensity at the Fermi energy. The sample alignment and the K-point position were calibrated with LEED and spin-integrated ARPES scans. Photon energies ranging from 30 eV to 55 eV were used for the measurements, and no significant photon energy dependence was found within the limited set of photon energies used. However, this does not eliminate the possibility of a photon-energy-dependent final state effect in the SARPES process in this material. Only the SARPES spectra measured with 55 eV are shown in this paper.

3. Data and discussion

3.1. Spin-integrated spectra of 1 ML $MoSe_2$ and WSe_2

Figure 1 shows the overall electronic structure of 1 ML $MoSe_2$ and WSe_2 from the spin-integrated ARPES spectra along the Γ-K direction of the surface hexagonal Brillouin zone. The key features of the monolayer MX_2 electronic structures are clearly visible both in the energy-momentum intensity maps in figures 1(a) and (b) and the stacks of energy distribution curves (EDCs) in figures 1(c) and (d). First, there exists only a single branch of bands at the Γ-point. The number of branches of the Γ-point band increases following the number of layers [20, 21]. Second, there exists a clear splitting in the valence band at the K-point. The size of this splitting is much larger in WSe_2 ∼470 meV compared to that in $MoSe_2$ ∼180 meV, due to the stronger SOC induced by the heavier element W. Third, the band maximum at the Γ-point is located at a higher binding energy than that at the K-point, leaving the valence band maximum at the K-point. Combining this with the conduction band minimum being at the K-point in the unoccupied state [20, 21, 26], the 1 ML $MoSe_2$ and WSe_2 are direct band gap semiconductors.

In the following discussions regarding the SARPES data, we will focus mostly on the split valence band feature at the K-point, which is proposed to be spin polarized [17, 19, 20].

3.2. Spin-resolved spectra of 1 ML $MoSe_2$ and WSe_2

In figure 2, we present the SARPES data at the K-point of 1 ML $MoSe_2$ and WSe_2. We first show a schematic drawing of the experimental geometry along with the definition of the xyz coordinates in the sample reference frame in figure 2(a). The angle between the incident photon momentum and the outgoing electrons is fixed at 45°. Different k-points in the momentum space can be reached by rotating the samples on all three axes: tilt (around the x axis), polar (around the y axis), and azimuth (around the z axis). The spectra are measured with 55 eV photons with C + photon polarization unless otherwise noted.

The spin-resolved EDCs along with the polarization, which is the difference between the up-spin intensity and the down-spin intensity divided by the sum of the two, are presented for the x, y, and z directions for 1 ML $MoSe_2$ (figures 2(b)–(d)) and for 1 ML WSe_2 (figures 2(e)–(g)). One immediately notices that the major component of the spin polarization is along the z direction—the out-of-plane direction from the sample surface—while there exist slight in-plane components that cannot be explained by simple experimental uncertainty. This is particularly clear in the WSe_2 case, in which the splitting between two valence band peaks is large

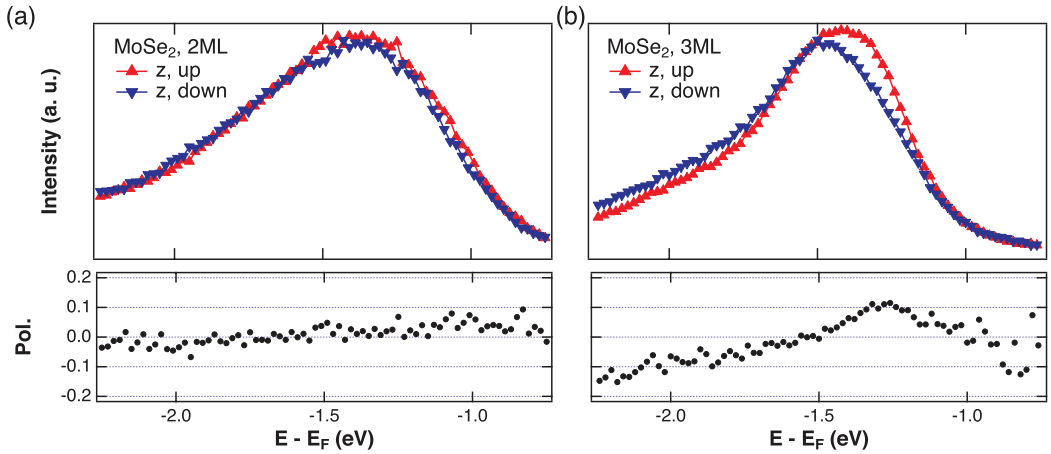

Figure 3. The SARPES spectra of 2 MLs and 3 MLs $MoSe_2$ at the K-point.

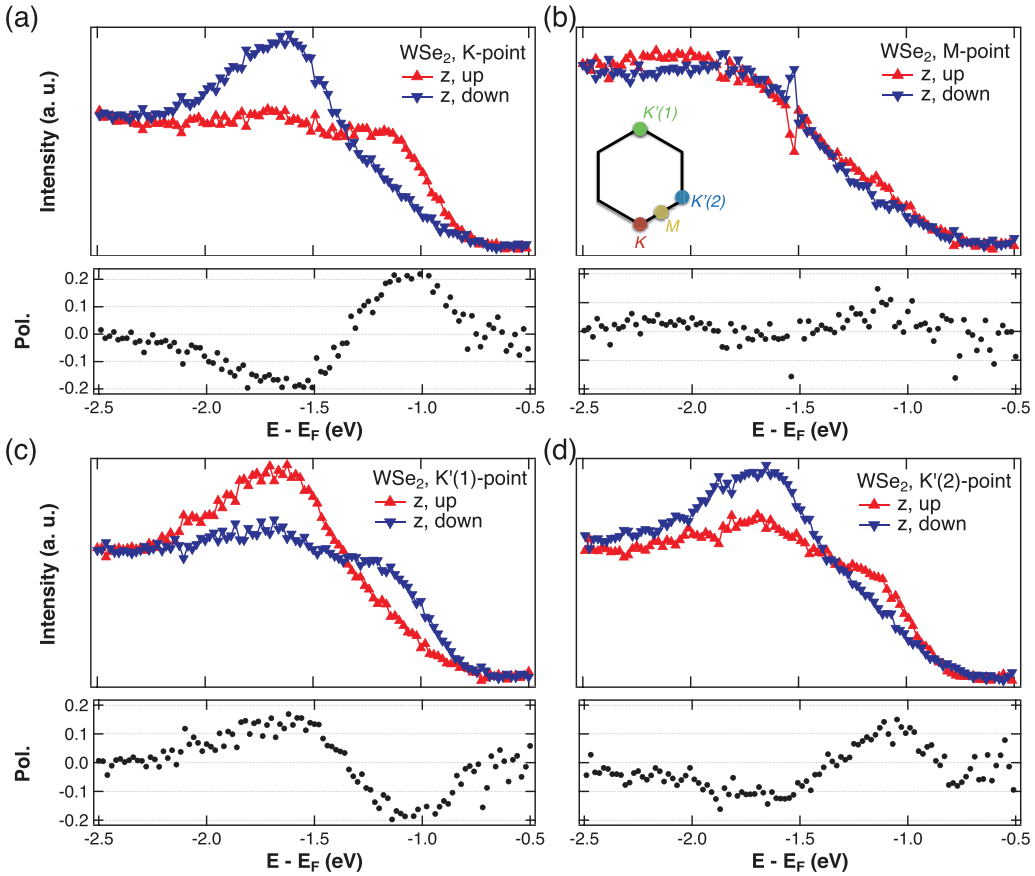

Figure 4. (a)–(d) Momentum dependence of the spin-resolved EDCs and the spin polarization of 1 ML WSe_2 at K, M, and K′(1) and K′(2) points. The inset in panel (b) shows a schematic illustration of the hexagonal Brillouin zone and the definition of the K, M, K′(1) and K′(2) points.

enough to overcome the inevitable limited resolution of the SARPES data. The intrinsic inefficiency of the SARPES process forced us to use a less collimated synchrotron light to allow the maximum amount of photons to reach the sample, which is translated into poorer resolution from the beamline compared to the spin-integrated ARPES, as well as a large spot size in the sample. For $MoSe_2$, the spin polarization is not as clear as that in WSe_2, as 180 meV splitting is now comparable to the energy resolution of the measurement; however, the polarization along the z direction—particularly for the lower binding energy peak ~ -1.4 eV—is still identifiable. Having the major component of spin polarization along the z direction is consistent with the previously reported SARPES work on bulk WSe_2 [39].

In theory [17, 19, 20], we only expect to see the spin polarization along the z direction at the K-point valence band maximum. The observed small amount of in-plane component indicates the existence of spin state interference [41] between

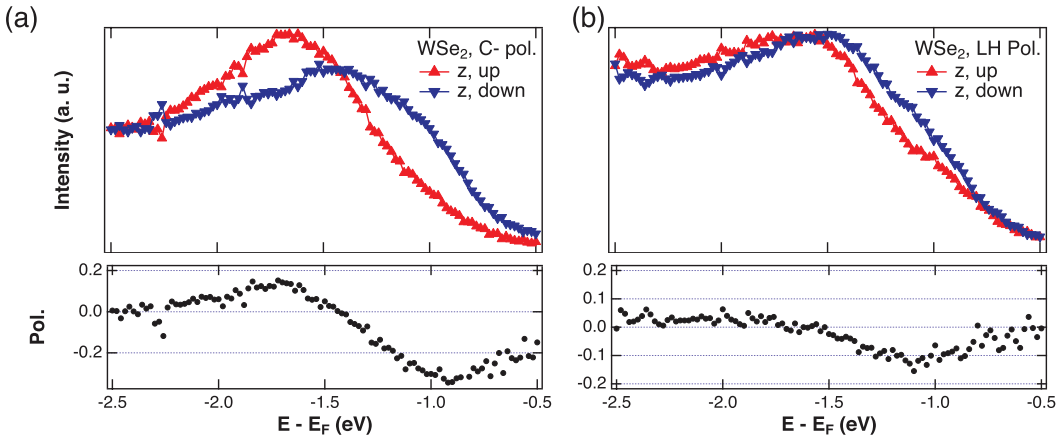

Figure 5. The photon polarization dependence of SARPES data from 1 ML WSe_2.

the different spin states of the K-point split bands, which can give a non-zero spin component along the x and y direction for the measured spin texture in SARPES. A similar effect is commonly observed in SARPES measurements, such as in the surface state of the Rashba alloy Sb/Ag(1 1 1) [41] and the topological surface state of Bi_2Se_3 [42].

Another interesting aspect of our SARPES data is that the maximum amount of polarization is only ∼20%, even in WSe_2 where clear separation between the spin-polarized peaks exists, as opposed to the nearly 100% expected from theoretical calculations [20]. We attribute this mainly to the limited resolution and the intrinsic broadening inherent in SARPES, which gives an overlap of the two spin-polarized states to reduce the measured spin polarization. Another contributing factor is the spin-independent or unpolarized background, due to the secondary scattering of the photoelectrons, which also decreases the measured spin polarization.

We also need to consider the existence of mirror twin domains, universal in MX_2 samples. Single layer MX_2 has 3-fold rotational symmetry, since M and X atoms occupy alternating hexagonal corners at different heights. The growth process therefore naturally favors triangular domains, as is clearly shown in the samples grown by CVD and the nanoparticles of MX_2 [43, 44]. Our samples grown by MBE are bound to have a mixture of domains with triangles pointing up (up-triangle domain) and its mirror twin domain pointing downwards (down-triangle domain), since they are energetically degenerate. Although such a mirror twin domain has interesting properties at the boundary [45, 46], it also acts to reduce the measured polarization in SARPES, since the signal from the K-point always mixes with that from the K′-point.

3.3. Thickness dependence of spin ARPES in $MoSe_2$

Now we move on to the thickness dependence of the SARPES spectra in $MoSe_2$ thin film samples. Since we have established that the major spin polarization component is along the z direction, we will only compare the z component of the SARPES data and spin polarization in subsequent sections.

Spin-resolved EDCs and spin polarization at the K-point along the z direction are shown in figure 3 for 2 MLs and 3 MLs $MoSe_2$. As the thickness increases from 1 ML (shown in figure 2(d)) to 2 and 3 MLs, we find that the spin polarization along the z direction disappears for 2 MLs but reappears in 3 MLs along the same direction. It has been theoretically proposed [20] that such oscillatory behavior would occur as the inversion symmetry is restored in 2 MLs and gets broken again for 3 MLs. However, the degree of polarization should decrease quite a bit in 3 MLs compared to 1 ML. This is not clearly observable in our data in figure 3(b) compared to figure 2(d), which is again due to the limited resolution and intrinsic broadening against the small splitting energy.

3.4. Crystal orientation dependence of the spin polarization

In this section, we discuss the key aspect of the spin-valley coupling in MX_2, which is the change in the spin polarization direction in the spin split valence band for different valleys, i.e. the spin flip between the K- and K′-point.

Figure 4 shows the momentum dependence of the spin-resolved EDCs and spin polarization along the z direction in 1 ML WSe_2. Figure 4(a) is an exact reproduction of the data already shown in figure 2(g), which shows up-spin polarization for the low-energy peak ~ -1.1 eV and down-spin polarization for the high-energy peak ~ -1.57 eV. Figure 4(b) is the SARPES data along the z direction at the M-point, which clearly shows no spin polarization. The inset in figure 4(b) is the schematic drawing to show the definition of the K, M, K′(1) and K′(2) points. From the center of the Brillouin zone, the Γ-point, the K- and the K′(1)-points can be accessed by changing the tilt angles. From the K-point, this requires the rotation of the azimuthal angles to reach the M- and K′(2)-points.

The K′(1)-point shown in figure 4(c) shows a clear reversal of spin polarization. The low-energy peak ~ -1.1 eV now has down-spin polarization while the high-energy peak ~ -1.57 eV exhibits up-spin polarization. Such a spin flip is expected from the strong spin-valley locking of MX_2 [15–17] and is considered to be a crucial aspect of valleytronic applications. On the other hand, the spin polarization at the K′(2)-point, reached by the azimuthal rotation from the K-point, shown in figure 4(d), does not show such spin flipping.

This apparent discrepancy between the two supposedly equivalent momentum points clearly indicates that there exists

a non-trivial geometric effect in our SARPES data. The change in flip angle involves the reversal of certain orbital parities with respect to the mirror plane defined by the incoming light and outgoing electron momentum, followed by the changes in the sign of the SARPES matrix element [47]. The reversal of the measured spin polarization by changing the flip angle suggests that the spin texture prominent in our measurement condition, 55 eV, C + polarized, is sensitive to the orbitals that change their parity when reflected with respect to the mirror plane. According to the first principle calculations [19, 39], the orbital character of the K-point VB is mainly in-plane, a mixture of d_{xy} and $d_{x^2-y^2}$, from which we expect the change of signs with the change in flip angle in our measurement geometry. A more detailed study of the spin texture depending on the orbital characters, in both theory and experiment, as was done for the topological surface state in topological insulators [48, 49], is necessary to disentangle the nature of measured spin texture in SARPES with respect to the initial state spin.

3.5. Photon polarization dependence of the spin ARPES data

Another important aspect to consider in SARPES measurements is the polarization of the incidence photons. Figure 5 shows the photon polarization dependence of the SARPES data on 1 ML WSe_2 at the K-point along the z direction. In figure 5(a), one can immediately notice that the spin polarization is reversed for the C- polarization of the incident photons, compared to that of the C+ photon polarization presented in figure 4(a). We observe a clear spin flip depending on the direction of rotation of the circularly polarized light. For incident photons with linear horizontal polarization, shown in figure 5(b), the spin polarization stays with the C- photon polarization, although it is less pronounced, particularly for the low binding energy peak.

Such a spin flip with the reversal of circular light polarization, along with the reduced degree of spin polarization with linear light polarization, may indicate that MX_2 could be another case for the control of photoelectron spin polarization through a change of incoming photon polarization, as shown for the topological surface state [42, 50, 51]. Such changes in spin polarization also strengthen the discussion in the previous section regarding the geometric effect due to the orbital selection rule and SARPES matrix element. As the incoming light polarization changes, the SARPES process selects only the spin polarization for the outgoing photoelectrons allowed by the orbital character and associated spin texture [51]. This can result in a dramatic effect, particularly for circularly polarized light, for which the measured spin polarization can completely flip its signs.

At the same time, we also need to consider that systems with strong SOC show a large intensity difference as the circular polarization of light is reversed [52]. This results in a particularly interesting case for Rashba systems [53], in which such circular dichroisms in the ARPES signal could provide important information on the orbital angular momentum of the system. After all, the spin split VB of MX_2 is due to the combination of inversion symmetry breaking and strong SOC, and the spin and orbital degrees of freedom are intricately intertwined. We cannot rule out that the observed flip of the polarization in our data is largely due to the circular dichroism, yet such a dichroism could also be closely related to the initial state spin texture. Further studies on circular dichroic ARPES intensity from WSe_2 and $MoSe_2$ with varying photon energies are required in order to fully understand and disentangle the close relationship between the spin and orbital in this system and in our SARPES data.

4. Conclusion

In conclusion, we have made SARPES measurements on some few-layer samples of $MoSe_2$ and WSe_2 grown by MBE on a bilayer graphene substrate. The spin polarization is mostly found to lie in the out-of-plane direction with respect to the sample surface, with a small amount of in-plane components. The amount of spin polarization is much smaller than what was theoretically proposed due to the limited resolution and overlap of two spin split states. With an increasing thickness, the measured spin polarization disappears in 2 MLs but reappears in 3 MLs as inversion symmetry is recovered and broken again, respectively. We found the flipping of spin polarization for different valleys with geometric dependence and strong light polarization dependence, which reveals the close coupling between orbital and spin degrees of freedom and the non-trivial nature of interpreting the SARPES data.

Acknowledgments

The work at ALS is supported by the US DOE, Office of Basic Energy Science, under contract no. DE-AC02-05CH11231. The work at the Stanford Institute for Materials and Energy Sciences and Stanford University is supported by the US DOE, Office of Basic Energy Sciences, under contract no. DE-AC02-76SF00515. The work at Pusan National University is supported by the National Research Foundation of Korea (NRF) funded by the Ministry of Science, ICT, and Future Planning (no. 2015R1C1A1A01053065). The work at the EPFL is supported by the Swiss National Science Foundation (PP00P2_144742/1).

References

[1] Geim A 2009 *Science* **324** 1530
[2] Service R F 2015 *Science* **348** 490
Gibney E 2015 *Nature* **522** 274
[3] Xu M, Liang T, Shi M and Chen H 2013 *Chem. Rev.* **113** 3766
[4] Chhowalla M, Shin H S, Eda G, Li L-J, Loh K P and Zhang H 2013 *Nat. Chem.* **5** 263
[5] Ohta T, Bostwick A, Seyller T, Horn K and Rotenberg E 2006 *Science* **313** 951
[6] Kim J, Baik S S, Ryu S H, Sohn Y, Park S, Park B-G, Denlinger J, Yi Y, Choi H J and Kim K S 2015 *Science* **349** 723
[7] Conley H J, Wang B, Ziegler J I, Haglund R F, Pantelides S T and Bolotin K I 2013 *Nano Lett.* **13** 3626

[8] Geim A K and Grigorieva I V 2013 *Nature* **499** 419
[9] Wang E *et al* 2013 *Nat. Phys.* **9** 621
[10] Splendiani A, Sun L, Zhang Y, Li T, Kim J, Chim C-Y, Galli G and Wang F 2010 *Nano Lett.* **10** 1271
[11] Mak K F, Lee C, Hone J, Shan J and Heinz T F 2010 *Phys. Rev. Lett.* **105** 136805
[12] Ugeda M M *et al* 2014 *Nat. Mater.* **13** 1091
[13] Ye Z, Cao T, O'Brien K, Zhu H, Yin X, Wang Y, Louie S G and Zhang X 2014 *Nature* **513** 214
[14] Chernikov A, Berkelbach T C, Hill H M, Rigosi A, Li Y, Aslan O B, Reichman D R, Hybertsen M S and Heinz T F 2014 *Phys. Rev. Lett.* **113** 076802
[15] Mak K F, He K, Shan J and Heinz T F 2012 *Nat. Nanotechnol.* **7** 494
[16] Zeng H, Dai J, Yao W, Xiao D and Cui X 2012 *Nat. Nanotechnol.* **7** 490
[17] Xiao D, Liu G-B, Feng W, Xu X and Yao W 2012 *Phys. Rev. Lett.* **108** 196802
[18] Mak K F, McGill K L, Park J and McEuen P L 2014 *Science* **344** 1489
[19] Zhu Z Y, Cheng Y C and Schwingenschlogl U 2011 *Phys. Rev.* B **84** 153402
[20] Zhang Y *et al* 2014 *Nat. Nanotechnol.* **9** 111
[21] Zhang Y *et al* 2016 *Nano Lett.* **16** 2485
[22] Britnell L *et al* 2013 *Science* **340** 1311
[23] Radisavljevic B, Radenovic A, Brivio J, Giacometti V and Kis A 2011 *Nat. Nanotechnol.* **6** 147
[24] Lopez-Sanchez O, Lembke D, Kayci M, Radenovic A and Kis A 2013 *Nat. Nanotechnol.* **8** 497
[25] Damascelli A, Hussain Z and Shen Z X 2003 *Rev. Mod. Phys.* **75** 473
[26] Eknapakul T *et al* 2014 *Nano Lett.* **14** 1312
[27] Alidoust N *et al* 2014 *Nat. Commun.* **5** 4673
[28] Latzke D W, Zhang W, Suslu A, Chang T-R, Lin H, Jeng H-T, Tongay S, Wu J, Bansil A and Lanzara A 2015 *Phys. Rev.* B **91** 235202
[29] Jin W *et al* 2013 *Phys. Rev. Lett.* **111** 106801
[30] Miwa J A, Ulstrup S, Sørensen S G, Dendzik M, Čabo A G, Bianchi M, Lauritsen J V and Hofmann P 2015 *Phys. Rev. Lett.* **114** 046802
[31] Osterwalder J 2012 *J. Phys.: Condens. Matter* **24** 171001
[32] Dil J H 2009 *J. Phys.: Condens. Matter* **21** 403001
[33] Heinzmann U and Dil J H 2012 *J. Phys.: Condens. Matter* **24** 173001
[34] Hsieh D *et al* 2009 *Science* **323** 919
[35] Jozwiak C *et al* 2011 *Phys. Rev.* B **84** 165113
[36] Sánchez-Barriga J *et al* 2014 *Phys. Rev.* X **4** 011046
[37] Suzuki R *et al* 2014 *Nat. Nanotechnol.* **9** 611
[38] Coy Diaz H, Bertran F, Chen C, Avila J, Rault J, Fèvre P, Asensio M C and Batzill M 2015 *Phys. Status Solidi* **9** 701
[39] Riley J M *et al* 2014 *Nat. Phys.* **10** 835
[40] Hoesch M, Greber T, Petrov V N, Muntwiler M, Hengsberger M, Auwrter W and Osterwalder J 2002 *J. Electron Spectrosc. Relat. Phenom.* **124** 263
[41] Meier F, Petrov V, Mirhosseini H, Patthey L, Henk J, Osterwalder J and Hugo Dil J 2011 *J. Phys.: Condens. Matter* **23** 072207
[42] Zhu Z H *et al* 2014 *Phys. Rev. Lett.* **112** 076802
[43] Li M-Y *et al* 2015 *Science* **349** 524
[44] Helveg S, Lauritsen J, Læ gsgaard E, Stensgaard I, Nørskov J, Clausen B, Topsøe H and Besenbacher F 2000 *Phys. Rev. Lett.* **84** 951
[45] Liu H *et al* 2014 *Phys. Rev. Lett.* **113** 066105
[46] Barja S *et al* 2016 *Nat. Phys.* **12** 751
[47] Landolt G 2014 Spin- and angle-resolved photoelectron spectroscopy on topological insulators and bulk Rashba systems *PhD Dissertation* Universität Zürich
[48] Zhang H, Liu C-X and Zhang S-C 2013 *Phys. Rev. Lett.* **111** 066801
[49] Cao Y *et al* 2013 *Nat. Phys.* **9** 499
[50] Jozwiak C *et al* 2013 *Nat. Phys.* **9** 293
[51] Park C-H and Louie S G 2012 *Phys. Rev. Lett.* **109** 097601
[52] Park S R *et al* 2012 *Phys. Rev. Lett.* **108** 046805
[53] Kim B *et al* 2013 *Phys. Rev.* B **88** 205408